



Research Article

# Combined thermionic emission and tunneling mechanisms for the analysis of the leakage current for $\text{Ga}_2\text{O}_3$ Schottky barrier diodes

A. Latreche<sup>1</sup> 

© Springer Nature Switzerland AG 2019

## Abstract

A new analysis method of reverse leakage current for  $\beta\text{-Ga}_2\text{O}_3$  Schottky barrier diodes is performed by using two models: bias dependence and no bias dependence of barrier height. The method incorporates both the current induced by the tunneling of carriers through the Schottky barrier and the current induced by the thermionic emission of carriers across the metal–semiconductor interface. The experimental reverse transition voltage between thermionic emission and tunneling process can be determined from the intersection of the two components that were separated from the total current. Below the reverse transition voltage, the thermionic emission current dominates, and above it, the tunneling current dominates, while near the reverse transition voltage, neither tunneling nor thermionic emission accurately describes the conduction process because the both currents have the same order of magnitude; therefore, the both mechanisms must be combined together. The experimental reverse transition voltage (bias-dependent model) increases for low and high temperatures and decreases at intermediate temperatures for  $\beta\text{-Ga}_2\text{O}_3$  Schottky barrier diodes. The bias dependence of the barrier height model shows that the barrier height is strongly dependent (increases) on the reverse bias, in particular at low temperatures and low reverse bias. This model can explain the discrepancy between the experimental characteristics and those calculated by no bias dependence of barrier height model.

**Keywords** Thermionic emission current · Tunneling current ·  $\beta\text{-Ga}_2\text{O}_3$  Schottky diode · Reverse transition voltage · Image force barrier lowering

## 1 Introduction

In recent years, the monoclinic beta phase of gallium oxide ( $\beta\text{-Ga}_2\text{O}_3$ ) is promising for next-generation power electronic devices because of its excellent material properties for high-voltage applications, e.g., a 4.8 eV bandgap, a breakdown field of 8 MV/cm, and a Baliga's figure of merit that is more than four times larger than those for SiC and GaN [1–7]. Moreover, it is available as high-quality freestanding  $\beta\text{-Ga}_2\text{O}_3$  substrates grown by inexpensive melt methods [7]. Several authors are conducting early-stage research on  $\beta\text{-Ga}_2\text{O}_3$ -based Schottky barrier diodes (SBDs). A few studies on  $\beta\text{-Ga}_2\text{O}_3$  SBDs

fabricated on  $\beta\text{-Ga}_2\text{O}_3$  single crystal grown by different growth methods with various crystal orientations have been reported in the literature [8–25]. Most of these studies investigated the electrical characteristics in forward bias conditions where the thermionic emission (TE) mechanism is predominant. Under reverse bias condition, undesirable large leakage currents have been observed for  $\beta\text{-Ga}_2\text{O}_3$  and large bandgap SBDs due to the high electric fields normally encountered in these devices, and hence, this effect can potentially limit operation in the reverse blocking mode as a result of excessive internal heating. It, therefore, becomes critical to analyze the origin of such reverse leakage currents and fundamentally

✉ A. Latreche, hlat26@yahoo.fr | <sup>1</sup>Département des sciences de la matière, Université de Bordj Bou Arreridj, Bordj Bou Arreridj, Algeria.



comprehend the underlying physics [26, 27]. Understanding of the various mechanisms contributing to leakage currents will allow, maybe, to improve the performance of these devices. In fact, the total current in a Schottky barrier diode under reverse bias is always made up of the sum of the two contributions by thermionic emission and tunneling process (thermionic field and field emission). However, traditionally, the different regimes of electron transport: thermionic emission and tunneling, are considered separately for analyzing the reverse characteristics  $I$ - $V$  of  $\beta$ -Ga<sub>2</sub>O<sub>3</sub> SBDs [12, 18], since they all appear at different conditions and can be exploited independently. In our more recent theoretical study [28], we investigated the conduction mechanisms of the reverse leakage current for 4H-SiC SBDs; we have found that the reverse transition voltage between TE mechanism and tunneling process is strongly dependent on temperature, barrier height, doping concentration, and effective mass. The purpose of the present article is to present precisely a simple analysis of the different contributions to the experimental net leakage current of  $\beta$ -Ga<sub>2</sub>O<sub>3</sub> SBDs. To this end, we propose a combined model for the leakage current of  $\beta$ -Ga<sub>2</sub>O<sub>3</sub> SBDs which takes into account in a common framework the two main sources of leakage current present in Schottky diodes, namely the current due to the thermionic emission of carriers across the Schottky barrier and the current due to the tunneling of carriers through the Schottky barrier. This method will allow us to separate the two components of the total current; hence, we can determine the experimental reverse transition voltage between the two contributed mechanisms.

## 2 Theory and modeling

The net current density across the metal–semiconductor interface is the algebraic sum of the two components: the electron current density  $J_{SM}$  from semiconductor to metal and vice versa,  $J_{MS}$ . The current from semiconductor to metal  $J_{SM}$  is proportional to the quantum transmission coefficient  $T(E_x)$  multiplied by the occupation probability in the semiconductor and the unoccupied probability in the metal [29]. A similar expression can be obtained for the metal–semiconductor current density  $J_{MS}$ , which traverses in the opposite direction. The net current density  $J_{Tot}$  is then given by [27–32]

$$J_{Tot} = J_{SM} - J_{MS} = \frac{A^*T}{k_B} \int_0^\infty T(E_x)N(E_x)dE_x \tag{1}$$

where  $k_B$  is the Boltzmann constant,  $T$  is the temperature,  $A^*$  is the effective Richardson constant, and  $N(E_x)$  is the supply function which is defined as

$$N(E_x) = \int_0^\infty (f_M(E) - f_S(E))dE_{||} \tag{2}$$

$$= \ln \left( \frac{1 + \exp(-q\zeta - E_x)/k_B T}{1 + \exp(-q\zeta - qV_R - E_x)/k_B T} \right)$$

The total energy  $E$  is the sum of a transversal component  $E_p$  parallel to the Schottky interface and a transversal component  $E_x$ .  $f_S$  and  $f_M$  are the Fermi–Dirac distribution functions for the semiconductor and the metal, respectively. In expression (2),  $\zeta$  denotes a difference between the equilibrium Fermi level and conduction bands. Our calculations are performed by using a Wentzel–Kramers–Brillouin (WKB) approximation of the tunneling probability  $T(E_x)$ . WKB approximation is known by its reasonable accuracy for calculating the tunneling probability through a reverse-biased Schottky barrier [33] and is expressed as

$$T_{WKB}(E_x) = \exp \left[ -2 \int_{x_1}^{x_2} \left( \frac{2m^*}{\hbar^2} (U(x) - E_x) \right)^{1/2} dx \right] \tag{3}$$

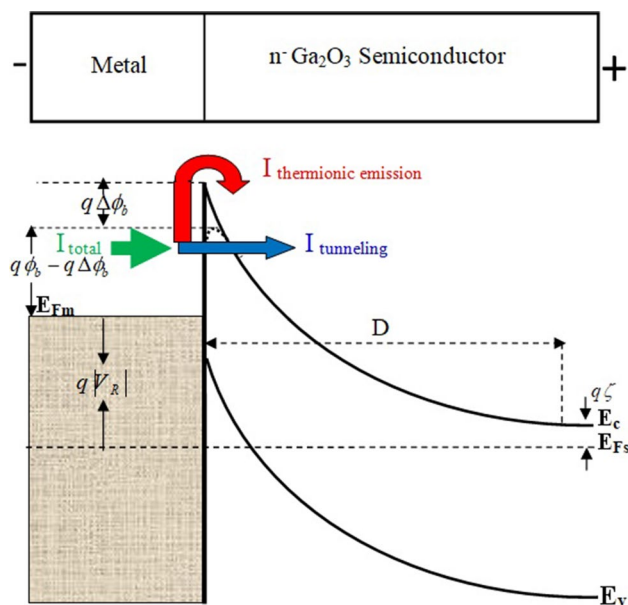


**Fig. 1** Energy band diagram of a metal/ $n$ -Ga<sub>2</sub>O<sub>3</sub> Schottky barrier diode under reverse bias. Electrons may overcome the barrier in two ways via thermionic emission (TE) (carriers pass over the barrier, red arrow) and tunneling process (carriers can tunnel through a potential barrier, blue arrow). The total current is the sum of the two components (green arrow). The arrows in the figure show the direction of the carriers, and the direction of the currents is the opposite. The effect of the image barrier lowering is included

where  $x_1$  and  $x_2$  are the two classical turning points. As shown in Fig. 1, the  $U(x)$  is the potential energy profile, for an arbitrary Schottky diode as measured with respect to the energy of the bottom of the conduction band in the bulk of the semiconductor, and it can be given by [27, 34]:

$$U(x) = \frac{q^2 N_D}{2\epsilon_S} (D - x)^2 - \frac{q^2}{16\pi\epsilon_S x} \tag{4}$$

where  $\epsilon_S$  is the semiconductor permittivity,  $D$  is the depletion width, and  $N_D$  is the doping concentration. The second term in Eq. (4) is the barrier lowering due to the image force effect. We note that the current expression (1) self-consistently includes both the process of conduction of carriers, i.e., tunneling for the lower energy range ( $E_x < U_{max}$ ), and TE mechanism for the higher energy range ( $E_x > U_{max}$ ) [27].

$$J_{Tot} = J_{Tun} + J_{Therm} \tag{5}$$

Here the component of reverse tunneling current density  $J_{Tun}$  can be expressed as [27, 31–34]

$$J_{Tun} = \frac{A^* T}{k_B} \int_0^{U_{max}} T(E_x) \ln \left( \frac{1 + \exp(-q\zeta - E_x)/k_B T}{1 + \exp(-q\zeta - qV_R - E_x)/k_B T} \right) dE_x, \tag{6}$$

and the component of TE current density  $J_{Therm}$  can be expressed as [27]

$$J_{Therm} = \frac{A^* T}{k_B} \int_{U_{max}}^{\infty} T(E_x) \ln \left( \frac{1 + \exp(-q\zeta - E_x)/k_B T}{1 + \exp(-q\zeta - qV_R - E_x)/k_B T} \right) dE_x. \tag{7}$$

For the energies  $E_x > U_{max}$  that correspond to the TE mechanism, the tunneling probability is equal to unity. Including the barrier lowering model and approximating the Fermi–Dirac statistics with the Maxwell–Boltzmann, Eq. (7) can be formulated as [27]

$$J_{Therm} = A^* T^2 e^{-\frac{q}{k_B T}(\phi_b - \Delta\phi_b)} \left( e^{\frac{qV_R}{k_B T}} - 1 \right) \tag{8}$$

where  $\Delta\phi_b$  is the barrier lowering due to the image force lowering effect, and it is given by [35]:

$$\Delta\phi_b = \left[ \frac{q^3 N_D (\phi_b - \zeta - V_R)}{8\pi^2 \epsilon_S^3} \right]^{1/4} \tag{9}$$

For extracting the barrier height ( $\phi_b$ ) from the reverse characteristic  $I$ – $V$ , we propose two models: The first model assumes that the barrier height  $\phi_b$  is assumed to be bias dependent due to the presence of an interfacial layer and interface states located between metal and semiconductor contact [36, 37].

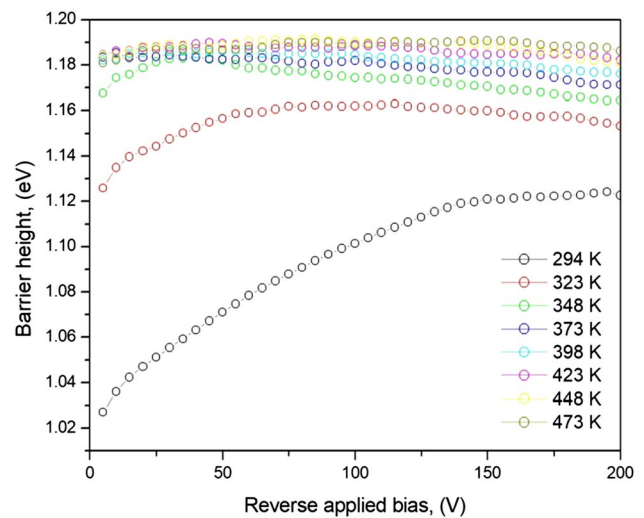


Fig. 2 Experimental Schottky barrier height as a function of the reverse bias voltage at various temperatures for  $\beta$ -Ga<sub>2</sub>O<sub>3</sub> SBD by solving numerically Eq. (10) for each bias voltage measurement

For that, we can solve numerically the following equation by Newton’s method.

$$J_{theor}^j(V_j) = J_{Tun}^j(V_j) + J_{Therm}^j(V_j) = J_{exp}^j(V_j) \tag{10}$$

where  $J_{exp}^j(V_j)$  is the reverse current density for each bias voltage measurement,  $J_{Tun}^j(V_j)$  and  $J_{Therm}^j(V_j)$  are the theoretical components of the current given by Eqs. (6) and (8), respectively.

The second model assumes that the effective barrier height is independent of the applied bias, and it can be determined from the first model by calculating the average value of the barrier height values calculated for each bias voltage measurement.

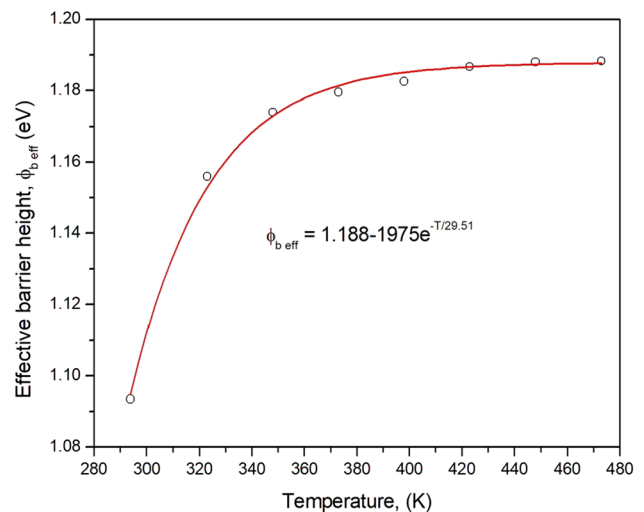
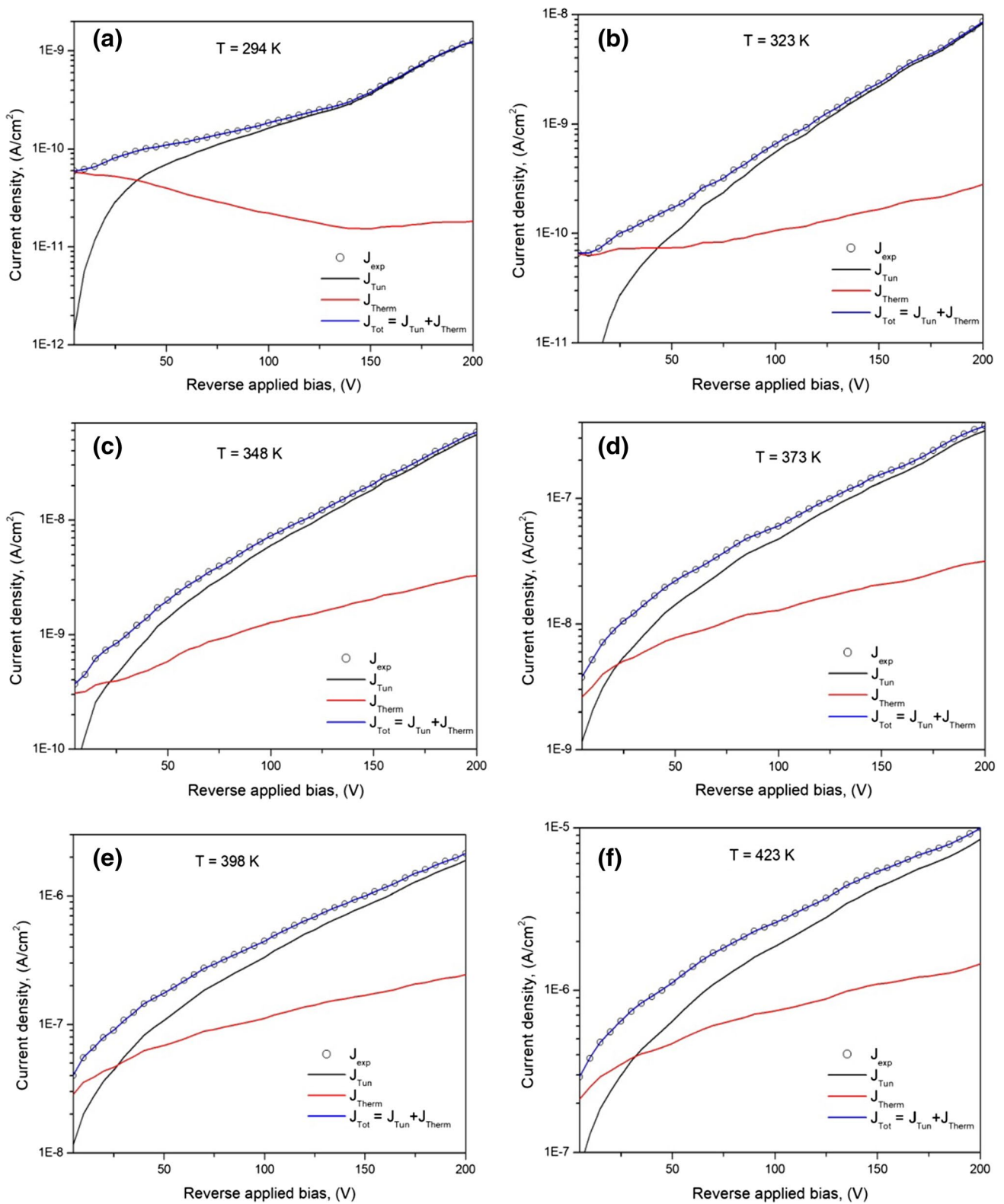


Fig. 3 Effective barrier height as a function of temperature for  $\beta$ -Ga<sub>2</sub>O<sub>3</sub> SBD



**Fig. 4** Reverse  $I$ - $V$  characteristics based on both the thermionic emission and the tunneling process for  $\beta\text{-Ga}_2\text{O}_3$  SBD for various temperatures. Experimental data are also shown. The calculated  $I$ - $V$  characteristics are resulting by using the extracted barrier height plotted in Fig. 2

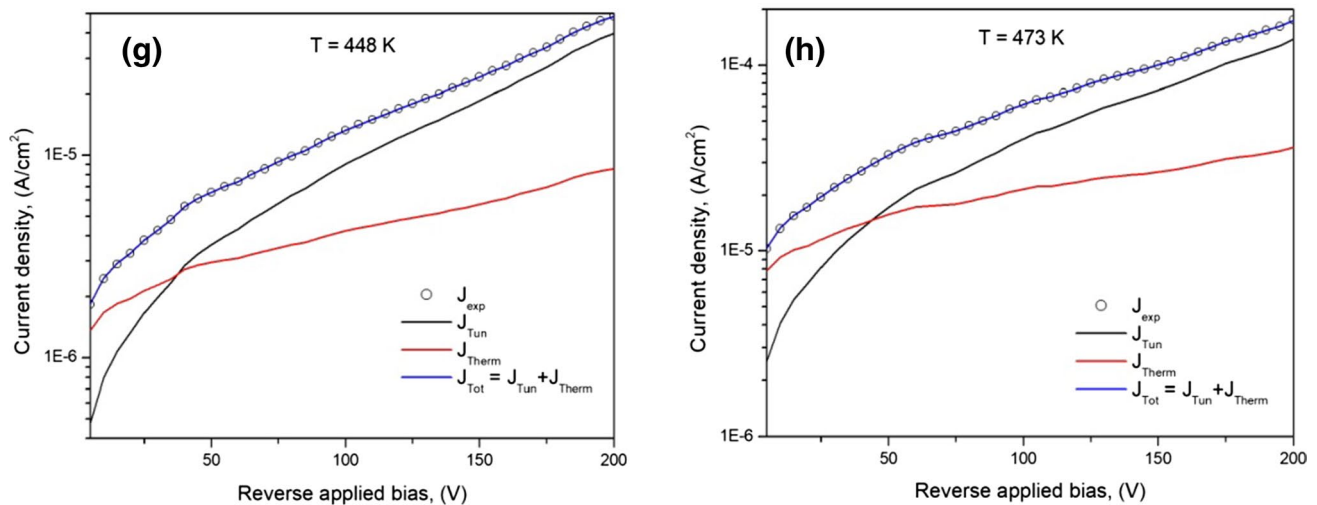


Fig. 4 (continued)

### 3 Results and discussion

In order to present our new proposed method, we used experimental data obtained with a Pt Schottky barrier diode on n-type  $\beta\text{-Ga}_2\text{O}_3$  (001) previously published by Higashiwaki et al. [12]. In their experimental study, the doping concentration was  $1.2 \times 10^{16} \text{ cm}^{-3}$ . Using the effective masses  $m^* = 0.342m_0$  from [38], the Richardson constant ( $A^*$ ) is calculated to be  $41.1 \text{ A K}^{-1} \text{ cm}^{-2}$ .

Figure 2 shows the resulting barrier height as a function of the reverse bias for  $\beta\text{-Ga}_2\text{O}_3$  SBD at various temperatures when the both mechanisms are combined. It can be seen that the barrier height increases with an increase in temperature, and it is strongly dependent on the reverse bias, in particular, below the temperature 373 K where the barrier height increases with increasing reverse bias and then starts to decrease slightly. This dependence on reverse bias becomes weak at high temperatures (above 373 K).

In Fig. 3, we show the variation of the average barrier height with the temperature. In this model, we assume that the barrier height is independent of the reverse bias, and the average value is the effective barrier height  $\phi_{b,\text{eff}}$ . From Fig. 3, it can be seen that the effective barrier height increases exponentially with temperature. We note that for SiC SBDs the Schottky barrier height strongly depends on the reverse bias voltage, temperature, and doping concentration [39]. These dependences are due to the combination of the effects of the interfacial layer and interface states located at the interface between metal and semiconductor contact [39].

Figure 4 shows the calculated and experimental reverse current densities according to tunneling and thermionic

models for  $\beta\text{-Ga}_2\text{O}_3$  SBD at various temperatures. The calculated reverse current densities are obtained by using the extracted barrier height which is plotted in Fig. 2. The intersection between the components of thermionic emission and tunneling currents represents the reverse transition voltage ( $V_T$ ) between the both corresponding mechanisms. The thermionic emission (TE) component is seen to be dominant for voltages up to about  $V_T$ , while the tunneling mechanism becomes larger for bias values beyond  $V_T$ . Near the reverse transition voltage, neither tunneling nor thermionic emission accurately describes the conduction process because the both currents have the same order of magnitude, and therefore, the both mechanisms must be combined together. In this model, where the barrier height is extracted from each data ( $I-V$ ), the total current which presents the sum of the two components has the same value as the experimental current. However, if we use the model that the barrier height is independent of the bias voltage, the total current is in good agreement with the experimental data especially for higher temperatures (above 373 K) as shown in Fig. 5. The discrepancies between calculation and experiment become large at lower temperatures (294 K; see Fig. 5a). This observation was reported in several works in the literature [12, 26, 40, 41]. Because the calculated reverse characteristics are not in good agreement with the experimental reverse characteristics at the lower temperatures in the case of no bias dependence of barrier height (second model), we can conclude that the bias dependence of barrier height model seems more appropriate than the second model for analysis the reverse characteristics  $I-V$  of  $\beta\text{-Ga}_2\text{O}_3$  SBDs.

The experimental reverse transition voltage between the thermionic and tunneling currents for the two models is determined from the intersection of the  $I-V$  curves and

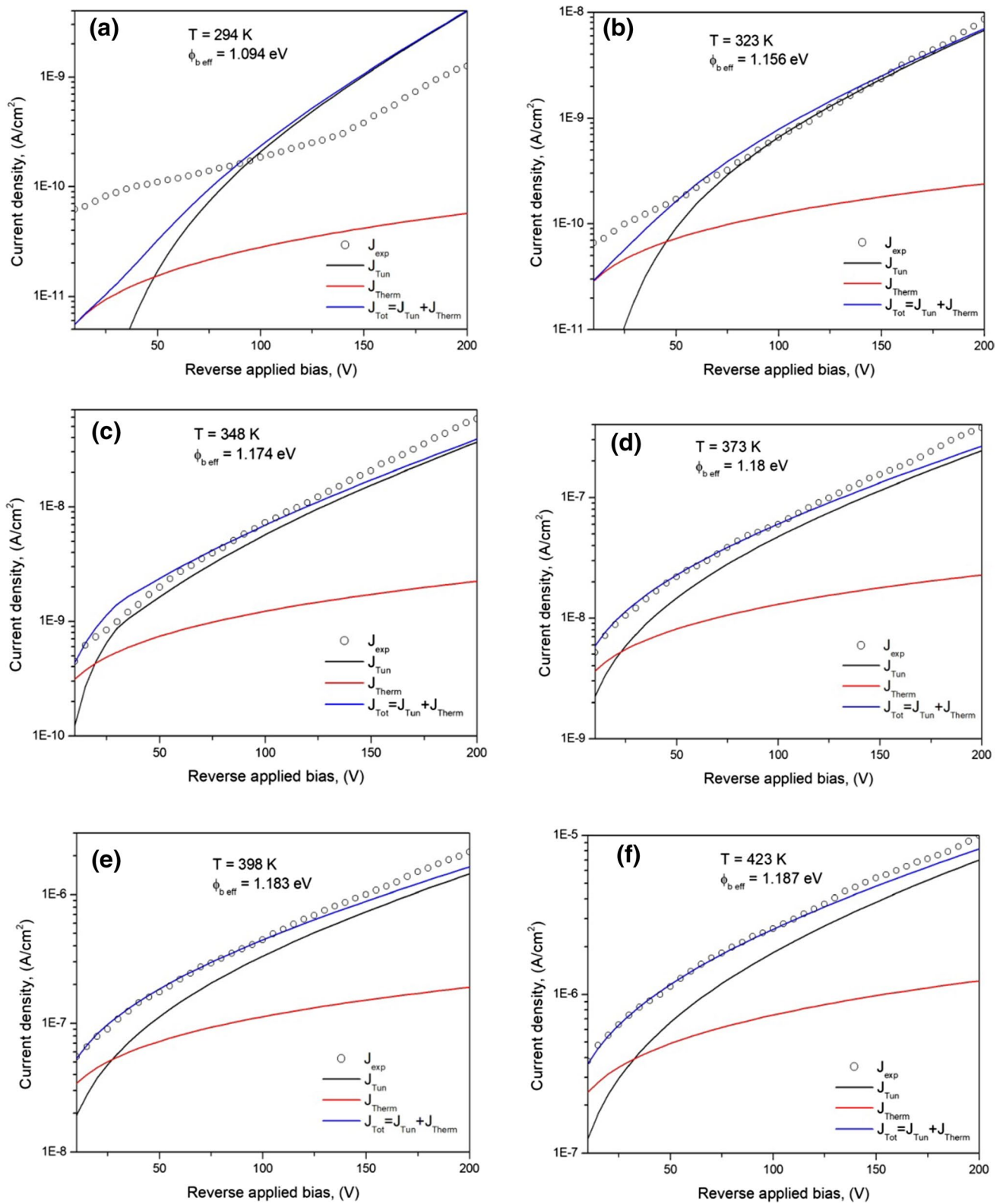


**Fig. 5** Reverse  $I$ - $V$  characteristics based on both the thermionic emission and the tunneling process for  $\beta$ -Ga<sub>2</sub>O<sub>3</sub> SBD for various temperatures. Experimental data are also shown. The calculated  $I$ - $V$  characteristics are resulting by using the extracted barrier height plotted in Fig. 3

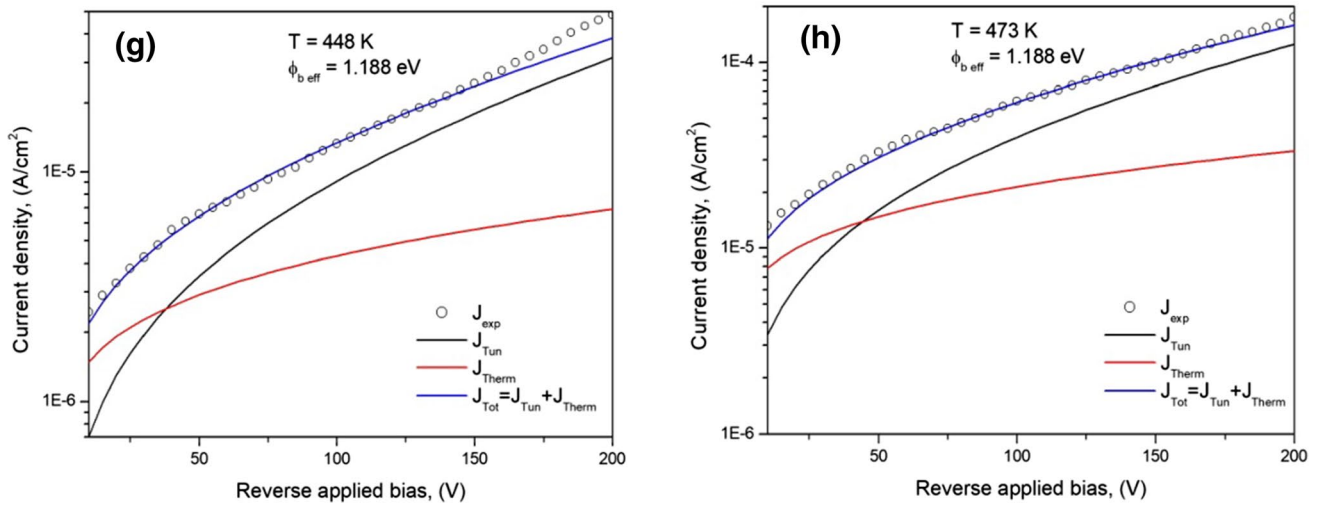


Fig. 5 (continued)

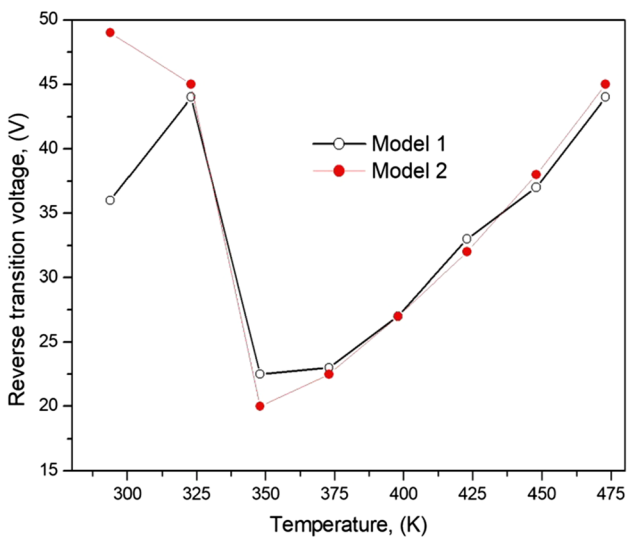


Fig. 6 Experimental reverse transition voltage as a function of temperature for  $\beta$ -Ga<sub>2</sub>O<sub>3</sub> Schottky barrier diode

plotted in Fig. 6. The values of the experimental reverse transition voltage for the two models are practically having the same values exception for temperature 294 K, and the reverse transition voltage has different values. As shown in Fig. 6, the reverse transition voltage is strongly dependent on the temperature. In the case of the first model, ( $\phi_b$  is assumed to be bias dependent), for example, the reverse transition voltage increases for temperatures below 323 K, and above 348 K, however, it decreases with increasing temperature for intermediate temperatures (223–348 K). This dependence of the experimental reverse transition voltage on temperature can be explained by

the competition between the TE and tunneling mechanisms when the reverse bias and temperature are changed simultaneously [28]. It seems to be well consistent with our recent proposed model for temperature dependence of reverse transition voltage of 4H-SiC SBDs [28]. Note that the tunneling and TE currents are increased either by increasing reverse bias or by increasing temperature, and the increase in the TE current is always smaller than the increase in tunneling current with increasing reverse bias. For low ( $T < 323$  K) and high ( $T > 348$  K) temperatures, the reverse bias should be increased to make the tunneling current component equal to the TE current component that is large compared with tunneling current component with increasing temperature. At the intermediate temperatures (223–348 K), the reverse bias should be decreased to make the tunneling component current equal to the TE current component that becomes smaller than the tunneling current component with increasing temperature.

### 4 Conclusion

Our study has been based upon a reverse current model which incorporates in a unified way both the current due to the thermionic emission of carriers across the metal–semiconductor interface and the tunneling current through the potential barrier. By means of the analytical method of the model, the different contributions to the net current of the  $\beta$ -Ga<sub>2</sub>O<sub>3</sub> Schottky barrier diode have been identified from experimental data  $I$ – $V$  previously published in the literature. The reverse transition voltage ( $V_T$ ) between thermionic emission and tunneling currents represents the value of the intersection of the

both curves  $I$ – $V$  of the two components. It has been shown that at low biases ( $V < V_T$ ) the current is dominated by the thermionic emission of carriers across the metal–semiconductor interface. At high biases ( $V > V_T$ ), the current is shown to be dominated by the tunneling of carriers through the potential barrier. The experimental reverse transition voltage increases for low and high temperatures, while for intermediate temperatures, the reverse transition voltage decreases with increasing temperature. Our treatment is done with the standard model (no bias dependence of barrier height) and also with bias dependence of barrier height model that maybe can explain the discrepancy between the experimental reverse characteristics and those calculated by the standard model for low temperatures.

### Compliance with ethical standards

**Conflict of interest** The author declares that they have no conflict of interest.

### References

- Zhang Z, Farzana E, Arehart AR, Ringel SA (2016) Deep level defects throughout the bandgap of (010)  $\beta$ - $\text{Ga}_2\text{O}_3$  detected by optically and thermally stimulated defect spectroscopy. *Appl Phys Lett* 108:052105. <https://doi.org/10.1063/1.4941429>
- Higashiwaki M, Sasaki K, Kuramata A, Masui T, Yamakoshi S (2012) Gallium oxide ( $\text{Ga}_2\text{O}_3$ ) metal–semiconductor field-effect transistors on single-crystal  $\beta$ - $\text{Ga}_2\text{O}_3$  (010) substrates. *Appl Phys Lett* 100:013504. <https://doi.org/10.1063/1.3674287>
- Fujita S (2015) Wide-bandgap semiconductor materials: for their full bloom. *Jpn J Appl Phys Part* 154:030101. <https://doi.org/10.7567/jjap.54.030101>
- Stepanov SI, Nikolaev VI, Bougrov VE and Romanov AE (2016) Gallium oxide: properties and applications—a review. *Rev Adv Mater Sci* 44:63–86. [http://www.ipme.ru/e-journals/RAMS/no\\_14416/06\\_14416\\_stepanov.html](http://www.ipme.ru/e-journals/RAMS/no_14416/06_14416_stepanov.html)
- Pearton SJ, Jiancheng Yang J, Cary PH IV, Ren F, Kim J, Tadger MJ, Mastro MA (2018) A review of  $\text{Ga}_2\text{O}_3$  materials, processing, and devices. *Appl Phys Rev* 5:011301. <https://doi.org/10.1063/1.5006941>
- Villora EG, Arjoca S, Shimamura K, Inomata D and Aoki K (2014)  $\beta$ - $\text{Ga}_2\text{O}_3$  and single-crystal phosphors for high-brightness white LEDs & LDs, and  $\beta$ - $\text{Ga}_2\text{O}_3$  potential for next generation of power devices. In Proceedings of SPIE 8987, oxide-based materials and devices V 89871U. <http://spie.org/Publications/Proceedings/Paper/10.1117/12.2039305>
- Kaun SW, Wu F, Speck JS (2015)  $\beta$ - $(\text{Al}_x\text{Ga}_{1-x})_2\text{O}_3/\text{Ga}_2\text{O}_3$  (010) heterostructures grown on  $\beta$ - $\text{Ga}_2\text{O}_3$  (010) substrates by plasma-assisted molecular beam epitaxy. *J Vac Sci Technol, A* 33:041508. <https://doi.org/10.1116/1.4922340>
- Sasaki K, Higashiwaki M, Kuramata A, Masui T and Yamakoshi S (2013)  $\text{Ga}_2\text{O}_3$  Schottky barrier diodes fabricated by using single-crystal  $\beta$ - $\text{Ga}_2\text{O}_3$  (010) substrate. *IEEE Electron Device Lett* 34:493–495. <https://ieeexplore.ieee.org/document/6471740>
- Oishi T, Koga Y, Harada K, Kasu M (2015) High-mobility  $\beta$ - $\text{Ga}_2\text{O}_3$  (201) single crystals grown by edge-defined film-fed growth method and their Schottky barrier diodes with Ni contact. *Appl Phys Express* 8:031101. <https://doi.org/10.7567/APEX.8.031101/meta>
- Jayawardena A, Ahyi AC, Dhar S (2016) Analysis of temperature dependent forward characteristics of Ni/( $_{201}$ )  $\beta$ - $\text{Ga}_2\text{O}_3$  Schottky diodes. *Semicond Sci Technol* 31:115002. <https://doi.org/10.1088/0268-1242/31/11/115002>
- Higashiwaki M, Sasaki K, Murakami H, Kumagai Y, Koukitu K, Kuramata A, Masui T, Yamakoshi S (2016) Recent progress in  $\text{Ga}_2\text{O}_3$  power devices. *Semicond Sci Technol* 31:034001. <https://doi.org/10.1088/0268-1242/31/3/034001>
- Higashiwaki M, Konishi K, Sasaki K et al (2016) Temperature-dependent capacitance–voltage and current–voltage characteristics of Pt/ $\text{Ga}_2\text{O}_3$  (001) Schottky barrier diodes fabricated on n- $\text{Ga}_2\text{O}_3$  drift layers grown by halide vapor phase epitaxy. *Appl Phys Lett* 108:133503. <https://doi.org/10.1063/1.4945267>
- Oh S, Yang G and Kim J (2017) Electrical characteristics of vertical Ni/ $\beta$ - $\text{Ga}_2\text{O}_3$  Schottky barrier diodes at high temperatures. *ECS J Solid State Sci Technol* 6:Q3022–Q3025. <http://jss.ecsdl.org/content/6/2/Q3022>
- Yao Y, Gangireddy R, Kim J, Das KK, Davis RF, Porter LM (2017) Electrical behavior of  $\beta$ - $\text{Ga}_2\text{O}_3$  Schottky diodes with different Schottky Metals. *J Vac Sci Technol, B* 35:03D113. <https://doi.org/10.1116/1.4980042>
- Ahmadi E, Oshima Y, Wu F, Speck JS (2017) Schottky barrier height of Ni to  $\beta$ - $(\text{Al}_x\text{Ga}_{1-x})_2\text{O}_3$  with different compositions grown by plasma-assisted molecular beam epitaxy. *Semicond Sci Technol* 32:035004. <https://doi.org/10.1088/1361-6641/aa53a7/meta>
- Farzana E, Zhang Z, Paul PK, Arehart AR, Ringel SA (2017) Influence of metal choice on (010)  $\beta$ - $\text{Ga}_2\text{O}_3$  Schottky diode properties. *Appl Phys Lett* 110:202102. <https://doi.org/10.1063/1.4983610?af=R>
- He Q, Mu W, Dong H, Long S, Jia Z, Liu HLQ, Tang M, Tao X, Liu M (2017) Schottky barrier diode based on  $\beta$ - $\text{Ga}_2\text{O}_3$  (100) single crystal substrate and its temperature-dependent electrical characteristics. *Appl Phys Lett* 110:093503. <https://doi.org/10.1063/1.4977766>
- Konishi K, Goto K, Murakami H, Kumagai Y, Kuramata A, Yamakoshi S, Higashiwaki M (2017) 1-kV vertical  $\text{Ga}_2\text{O}_3$  field-plated Schottky barrier diodes. *Appl Phys Lett* 110:103506. <https://doi.org/10.1063/1.4977857>
- Oshima T, Hashiguchi A, Moribayashi M, Koshi K, Sasaki K, Kuramata A, Ueda O, Oishi T, Kasu M (2017) Electrical properties of Schottky barrier diodes fabricated on (001)  $\beta$ - $\text{Ga}_2\text{O}_3$  substrates with crystal defects. *Jpn J Appl Phys* 56:086501. <https://doi.org/10.7567/JJAP.56.086501/meta>
- Yang J, Ren F, Khanna R et al (2017) Annealing of dry etch damage in metallized and bare (-201)  $\text{Ga}_2\text{O}_3$ . *J Vac Sci Technol, B* 35:051201. <https://doi.org/10.1116/1.4986300>
- Li A, Feng Q, Zhang J, Hu Z et al (2018) Investigation of temperature dependent electrical characteristics on Au/Ni/ $\beta$ - $\text{Ga}_2\text{O}_3$  Schottky diodes. *Superlattices Microstruct* 119:212–217. <https://www.sciencedirect.com/science/article/pii/S0749603618307250>
- He Q, Mu W, Fu B, Z. Jia Z et al (2018) Schottky barrier rectifier based on (100)  $\beta$ - $\text{Ga}_2\text{O}_3$  and its DC and AC characteristics. *IEEE Electron Device Lett* 39:556–559. <https://ieeexplore.ieee.org/abstract/document/8305486>
- Jian G, He Q, Mu W, Fu B et al (2018) Characterization of the inhomogeneous barrier distribution in a Pt/(100) $\beta$ - $\text{Ga}_2\text{O}_3$



- Schottky diode via its temperature-dependent electrical properties. *AIP Adv* 8:015316. <https://doi.org/10.1063/1.5007197>
24. Fu H, Chen H, Huang X, Baranowski I et al (2018) A comparative study on the electrical properties of vertical (2 0 1) and (010)  $\beta$ -Ga<sub>2</sub>O<sub>3</sub> Schottky barrier diodes on EFG single-crystal substrates. *IEEE Trans Electron Devices* 65:3507–3513. <https://ieeexplore.ieee.org/document/8376002>
  25. Yang J, Ren F, Tadjer M, Pearton SJ, Kuramata A (2018) Ga<sub>2</sub>O<sub>3</sub> Schottky rectifiers with 1 ampere forward current, 650 V reverse breakdown and 26.5 MW/cm. *AIP Adv* 8:055026. <https://doi.org/10.1063/1.5034444>
  26. Crofton J, Sriram S (1996) Reverse leakage current calculations for SiC Schottky contacts. *IEEE Trans Electron Devices* 43:2305–2307. <https://ieeexplore.ieee.org/document/544427>
  27. Furno M, Bonani F, Ghione G (2007) Transfer matrix method modelling of inhomogeneous Schottky barrier diodes on silicon carbide. *Solid-State Electron* 51:466–474. <https://www.sciencedirect.com/science/article/pii/S0038110107000676>
  28. Latreche A (2019) Conduction mechanisms of the reverse leakage current of 4H-SiC Schottky barrier diodes. *Semicond Sci Technol* 34:025016. <https://doi.org/10.1088/1361-6641/aaf8cb>
  29. Chang CY, Sze SM (1970) Carrier transport across metal–semiconductor barriers. *Solid-State Electron* 13:727–740. [https://doi.org/10.1016/0038-1101\(70\)90060-2](https://doi.org/10.1016/0038-1101(70)90060-2)
  30. Gehring A, Selberherr S (2004) Modeling of tunneling current and gate dielectric reliability for nonvolatile memory devices. *IEEE Trans Device Mater Reliab* 4:306–319. <https://doi.org/10.1109/TDMR.2004.836727>
  31. Eriksson J, Rorsman N, Zirath H (2003) 4H-silicon carbide Schottky barrier diodes for microwave applications. *IEEE Trans Microw Theory Technol* 51:796–804. <https://ieeexplore.ieee.org/document/1191732>
  32. Tsu R, Esaki L (1973) Tunneling in a finite superlattice. *Appl Phys Lett* 22:562–564. <https://doi.org/10.1063/1.1654509>
  33. Latreche A, Ouennoughi Z (2013) Modified Airy function method modeling of tunnelling current for Schottky barrier diodes on silicon carbide. *Semicond Sci Technol* 28:105003. <https://doi.org/10.1088/0268-1242/28/10/105003>
  34. Zheng L, Joshi RP, Fazi C (1999) Effects of barrier height fluctuations and electron tunneling on the reverse characteristics of 6H-SiC Schottky contacts. *J Appl Phys* 85:3701–3707. <https://doi.org/10.1063/1.369735>
  35. Rhoderick EH, Williams RH (1988) *Metal–semiconductor contact*. Oxford University Press, Oxford
  36. Naik SS, Reddy VR (2012) Temperature dependency and current transport mechanisms of Pd/V/n-type InP Schottky rectifiers. *Adv Mat Lett* 3:188–196. <https://www.vbripress.com/aml/articles/details/222>
  37. Turut A, Saglam M, Efeoglu H, Yalcin N, Yildirim M, Abay B (1995) Interpreting the nonideal reverse bias CV characteristics and importance of the dependence of Schottky barrier height on applied voltage. *Phys B Condens Matter* 205:41–50. [https://doi.org/10.1016/0921-4526\(94\)00229-0](https://doi.org/10.1016/0921-4526(94)00229-0)
  38. He H, Orlando R, Blanco MA, Pandey R (2006) First-principles study of the structural, electronic, and optical properties of Ga<sub>2</sub>O<sub>3</sub> in its monoclinic and hexagonal phases. *Phys Rev B* 74:195123. <https://doi.org/10.1103/PhysRevB.74.195123>
  39. Latreche A (2014) Reverse bias-dependence of Schottky barrier height on silicon carbide: influence of the temperature and donor concentration. *Int J Phys Res* 2:40–49. <https://doi.org/10.14419/ijpr.v2i2.3120>
  40. Oyama S, Hashizume T, Hasegawa H (2002) Mechanism of current leakage through metal/n-GaN interfaces. *Appl Surf Sci* 190:322–325. [https://doi.org/10.1016/S0169-4332\(01\)00902-3](https://doi.org/10.1016/S0169-4332(01)00902-3)
  41. Treu M, Rupp R, Kpels H, Bartsch W (2001) Temperature dependence of forward and reverse characteristics of Ti, W, Ta and Ni Schottky diodes on 4H-SiC. *Mater Sci Forum* 353–356:679–682. <https://doi.org/10.4028/www.scientific.net/MSF.353-356.679>

**Publisher's Note** Springer Nature remains neutral with regard to jurisdictional claims in published maps and institutional affiliations.